[7]S. T. Manson and J. W. Cooper, Phys. Rev. 165, 126 (1968).
[8]F. Combet Farnoux and Y. Heno, Compt. Rend. 264B, 138 (1967); F. Combet Farnoux, *ibid.* 264B, 1728 (1967).
[9]H. Hall, Rev. Mod. Phys. 8, 358 (1936).
[10]M. O. Krause, T. A. Carlson, and R. D. Dismukes, Phys. Rev. 170, 37 (1968).
[11]T. A. Carlson, Phys. Rev. 156, 142 (1967).
[12]J. W. Cooper and S. T. Manson, following paper, Phys. Rev. 177, 157 (1969).
[13]W. Bothe, in Handbuch der Physik (Springer-Verlag, Berlin, 1933), Vol. 23.2, and references therein.
[14]J. Berkowitz and H. Ehrhardt, Phys. Letters 21, 531 (1966); and J. Berkowitz, H. Ehrhardt, and T. Tekaat, Z. Physik 200, 69 (1967).
[15]Z. Sujkowski, Arkiv Fysik 20, 269 (1961).
[16]W. Bothe, Z. Physik 26, 59 (1924); C. T. R. Wilson, Proc. Roy. Soc. (London) Ser. A 104, 1 (1923); P. Auger, Compt. Rend. 188B, 447 (1929).
[17]E. C. Watson and J. A. van der Akker, Proc. Roy. Soc. (London) Ser. A 126, 138 (1930).
[18]M. O. Krause, Phys. Rev. 140, A1845 (1965).
[19]M. O. Krause and T. A. Carlson, Phys. Rev. 149, 52 (1966).
[20]In Fig. 3a the continuum near the Kr$M_{4,5}$(MgK_α) line contains, however, a small contribution from Kr$L_{2,3}$–M_1M_1 Auger lines, and in Fig. 2 some weaker photolines interfere.
[21]For a review see U. Fano and J. W. Cooper, Rev. Mod. Phys. 40, 441 (1968).
[22]Charge spectra reported in Ref. 19 can readily be recalculated with the present experimental values for multiple-electron ionization and for the various subshell contributions.
[23]F. W. Byron and C. J. Joachain, Phys. Letters 24A, 616 (1967), and Phys. Rev. 164, 1 (1967).
[24]Some determinations of relative subshell cross sections by the same method have recently been reported by K. Siegbahn, C. Nordling, A. Fahlman, R. Nordberg, K. Hamrin, J. Hedman, G. Johansson, T. Bergmark, S. Karlsson, I. Lindgren, and B. Lindberg, Nova Acta Reg. Soc. Sci. Upsaliensis Ser. 20, 1 (1967); J. A. R. Samson and R. B. Cairns [Phys. Rev. 173, 80 (1968)] used a retarding-potential method to determine subshell contributions.
[25]Preliminary data of the author on M and N subshell cross sections of Xe show satisfactory agreement with theoretical results of Ref. 7.
[26]An attempt in this direction has been made by U. Fano and J. W. Cooper (see Ref. 21).

PHYSICAL REVIEW VOLUME 177, NUMBER 1 5 JANUARY 1969

Photo-Ionization in the Soft X-Ray Range: Angular Distributions of Photoelectrons and Interpretation in Terms of Subshell Structure

John W. Cooper and Steven T. Manson*†
National Bureau of Standards, Washington, D. C. 20234
(Received 2 August 1968; revised manuscript received 25 October 1968)

The problem of determining the individual subshell contributions in atomic photoabsorption is discussed. The general form of the angular distribution of photoelectrons in the soft x-ray range for polarized and unpolarized incident photons is considered. Calculations of the subshell contributions within a central-field model and the angular distribution of electrons from these contributions for photoabsorption in Kr in the energy range 200–1500 eV are presented and found to show good agreement with the experimental results of the preceding paper.

I. INTRODUCTION

Absorption of radiation by atoms in the x-ray range is ordinarily considered as a two stage process. Radiation is absorbed and a single electron is emitted from one of the various subshells of the atom whose binding energy is less than the energy of the incident radiation. This initial photo-ionization process is followed by a rearrangement of the remaining electrons in the ionic core, accompanied by emission of fluorescent radiation or by secondary electrons. From this viewpoint absorption is considered as a single-electron process.

Direct measurements of the attenuation of radiation, while they provide absolute measurements of the absorption, provide no breakdown of the contributions of electrons from various subshells. However, such a breakdown can be obtained from direct measurements of the energy distribution of electrons following absorption. While this technique is not new,[1] it has seldom been applied to determine a breakdown of subshell contributions to photoabsorption. Theory, on the other hand, determines uniquely the various subshell contributions to photoabsorption when subshell structure is explicitly represented by the wave functions describing the atomic system. Recent work[2,3] has provided a breakdown into subshell contributions and has demonstrated that moderately good agreement with total absorption measurements may be obtained. However, the partitioning of the total absorption cross section into various subshell components has never been verified experimentally. The work described in the preceding paper[4] rep-

resents a step in this direction.

Actually the separation of the photoabsorption cross section into various subshell components is in itself an approximation valid only insofar as absorption is a single electron process. Experiments such as those of the preceding paper may thus be viewed in a broader framework as attempting to separate the part of the absorption which is due predominantly to single electron excitation from processes in which the excitation is shared between two or more electrons.

The problem of inferring cross sections for each subshell from measurements of ejected electrons implies either a measurement or estimate of their angular distribution, unless electrons are collected over the full 4π geometry. Actually the form of the angular distribution of photoelectrons in absorption processes at moderate photon energies is quite simple. Earlier work on the angular distribution of ejected electrons[5] focuses on the effects of retardation and relativistic corrections which become important at high incident photon energies. More recently a simple form for the angular distribution within the non-relativistic dipole approximation has been used to predict the angular distribution of electrons in photodetachment processes.[6] The form of the angular distribution of electrons emitted in photoabsorption processes actually is but a special case of the general problem of angular correlations, which has been treated in detail for nuclear reactions.[7] We will attempt here to relate these different viewpoints.

II. THEORY

A. General Form of the Angular Distribution of Photoelectrons for Polarized and Unpolarized Radiation

For a single-electron model it has been shown that for polarized incident light the angular distribution of ejected electrons will be of the form[8,9]

$$\frac{d\bar{\sigma}(\vec{K},I_t)}{d\Omega}=\frac{\bar{\sigma}(K,I_t)}{4\pi}[1+\beta P_2(\cos\phi)], \qquad (1)$$

where $\bar{\sigma}(K,I_t)$ is the total cross section for ionization of an electron with binding energy I_t and final momentum $\vec{K}$, and ϕ is the angle between the direction of polarization and the direction of outgoing electrons $\hat{K}$.

Equation (1) defines the angular distribution of photoelectrons relative to the direction of polarization of the incident light. Unpolarized light can be considered as the incoherent superposition of two polarized beams with one polarization direction lying in the plane defined by the incident photon ($\vec{K}_\nu$) and final electron ($\hat{K}$) directions, and the other perpendicular to it. For unpolarized light the angular distribution of ejected electrons will then be

$$\frac{d\bar{\sigma}(\vec{K},I_t)}{d\Omega}=\frac{\bar{\sigma}(K,I_t)}{4\pi}[1-\tfrac{1}{2}\beta P_2(\cos\theta)]$$

$$=A+B\sin^2\theta, \qquad (2)$$

where $\theta=\cos^{-1}(\hat{K}\cdot\hat{K}_\nu)$ is the angle between incident photon beam and the final electron direction.

Equations (1) and (2) may be obtained alternatively by considering the photoabsorption process with electron emission as a general scattering process involving photons and unoriented atoms initially and ions and free electrons finally:

$$h\nu+A\rightarrow A^+ +e. \qquad (3)$$

From this point of view, Eqs. (1) and (2) follow at once from results derived some years ago concerning the angular distribution of products in nuclear reactions. Yang[10] has shown that for unpolarized radiation the general form of the angular distribution in any reaction of the form of Eq. (3) will be that given by Eq. (2), provided the absorption occurs via an electric dipole process. The key points in this derivation are the following: (a) only one direction in space ($\vec{K}_\nu$) is specified before absorption takes place. This limits the form of the angular distribution of electrons to $d\bar{\sigma}/d\Omega=\sum_l a_l P_l(\cos\theta)$. (b) Odd values of l can only arise from interference between final states of opposite parity. For electric dipole absorption only final states of a single parity will be present, so that only even values of l can occur in the above expression. (c) When absorption takes place via an electric dipole process, the value of l in the above summation is restricted to $l=0,2$, and hence the angular distribution must be of the form of Eq. (2).[11] The analogous result of Eq. (1) is obtained by the same argument, except that now the only direction specified is the initial direction of polarization.[12]

The above considerations, although well known in nuclear physics, have been treated in some detail here since they have important implications on photoelectron spectroscopy. First, Eqs. (1) and (2) are general results which are valid for the angular distribution of any particle ejected as the result of electric dipole absorption.[13] They are thus valid for photoelectrons from atoms or molecules, Auger electrons, electrons which result from two-electron excitation, or ions or neutral particles which result from molecular ionization followed by dissociation. Deviations from the form of these equations implies the presence of absorption via processes other than electric dipole.

Second, the use of polarized light yields no new information about the absorption process. A single parameter [β of Eqs. (1) or (2)] is obtained from the measurement of the angular distribution of any particle at a given energy for both polarized and unpolarized incident monoenergetic light.

B. Total and Differential Cross Sections from a Given Subshell

Within a central-potential model the cross section for photo-ionization pertinent to a given subshell can be computed easily using the formulation of Ref. 3.[14] The cross section for the nlth complete subshell will be

$$\sigma_{nl}(\epsilon) = \tfrac{4}{3}\pi\alpha a_0^2(\epsilon + \epsilon_{nl})[l R_{\epsilon, l-1}^2 + (l+1)R_{\epsilon, l+1}^2]. \tag{4}$$

Here ϵ_{nl} is the binding energy for a single electron in the nlth subshell, and ϵ is the energy of the free electron in the final state. The factors $R_{\epsilon, l\pm1}$ are dipole radial integrals which depend on the radial wave functions for bound and free electrons;

$$R_{\epsilon, l\pm1} = \int_0^\infty P_{nl}(r) P_{\epsilon, l\pm1}(r) dr. \tag{5}$$

The one electron orbitals $P_{nl}(r)$ and $P_{\epsilon l}(r)$ are eigenfunctions of a given effective central potential appropriate to bound and free electrons. These orbitals satisfy the normalization conditions

$$\int_0^\infty P_{nl}^2(r) dr = 1, \tag{6}$$

$$P_{\epsilon l}(r) \to \epsilon^{-1/4} \sin[\epsilon^{1/2} r - \tfrac{1}{2} l\pi - \epsilon^{-1/2} \ln 2\epsilon^{1/2} r + \delta_l(\epsilon)], \quad \text{as } r \to \infty. \tag{7}$$

In a central-potential model the angular distribution of ejected electrons is also completely specified for each subshell. The differential cross section for polarized or unpolarized light will be of the form of Eq. (1) or (2) with $\beta(\epsilon)$ equal to[15]

$$\frac{l(l-1)R_{\epsilon, l-1}^2 + (l+1)(l+2)R_{\epsilon, l+1}^2 - 6l(l+1)R_{\epsilon, l+1}R_{\epsilon, l-1}[\delta_{l+1}(\epsilon) - \delta_{l-1}(\epsilon)]}{(2l+1)[l R_{\epsilon, l-1}^2 + (l+1)R_{\epsilon, l+1}^2]}, \tag{8}$$

where $R_{\epsilon, l\pm1}$ is given by Eq. (5) and the phase shifts $\delta_{l\pm1}$ by Eq. (7).

Equations (1), (2), (4) and (8) provide a complete prescription for determining both the total contribution of the photoabsorption cross section and its angular distribution within the framework of the central potential model of Ref. 3.

III. CALCULATIONS AND COMPARISON WITH EXPERIMENT

A. Total Cross Sections and Cross Sections at 90°

Using the methods described in Ref. 3 the photoionization cross section for each subshell of Kr has been calculated for incident photon energies of 100–1500 eV. The detailed results are shown in Fig. 1 along with available experimental evidence on total absorption in this range.[16] The agreement is about the same as that obtained for other calculations of this type[3,17]; i.e., the theory predicts a sharper peak than experiment at a lower energy. We expect the breakdown of the total cross section into subshell contributions as given by this calculation to be reasonably accurate (10–20%) even near the maximum of absorption, and more accurate at higher energies.

A detailed comparison of these results can be made with the data given in Fig. 2 of Ref. 4 by the following procedure. First, we assume that retardation effects are negligible and compute the cross section at 90° from the incident beam using Eqs. (2) and (8) for each incident photon energy and each subshell contributing. Next, since the source contains several spectral lines, we weight these contributions by the relative intensities of the various emission lines. Finally, we weight each contribution by electron energy since the electron spectrometer measures energy flux and not number flux. Our results are normalized to the largest peak in the experimental spectra, $M_{4,5}(L_\alpha)$. The computed values are plotted as lines proportional to the electron energy flux at 90°.[18]

The results are shown in Fig. 2. This comparison shows clearly that the labeled peaks are in fact due to single electron transitions and that the intensities of these peaks are in good agreement with our calculated results for individual subshell contributions. It also shows that the large contributions below the major peaks $M_{4,5}(L_\alpha)$ and $M_{2,3}(L_\alpha)$, as well as the "background" below ~650 eV, must be due to two-electron processes as stated in Ref. 4.

A direct comparison of the energy dependence of the various subshell contributions as measured and calculated may be made by plotting the ratio of the cross section for each subshell to the $M_{4,5}(3d)$ contributions at 90° as a function of energy.

Fig. 3 shows such plots based on the calculated cross sections and the data given in Table II of Ref. 4. The results indicate agreement between theory and experiment in both the value and the trend of these ratios as a function of energy. The experimental ratios are somewhat higher than we calculate at energies below 500 eV and lower at higher energies. This is consistent with a broadening and shift to higher energies of the $3d$ contribution.

B. Angular Distributions

With retardation neglected the angular distribution depends only on β in Eq. (2) or alternatively on $A + B\sin^2\theta$ as in Table II of Ref. 4, where $\beta = 4B/(3A + 2B)$. In Fig. 4 we show a comparison of β from our calculations with the data in Table II of Ref. 4, over the entire energy range included in our calculations. Also shown is the single point obtained for $4p$ electrons from a 584 Å source obtained in a previous measurement.[19] Several things are apparent from the data shown in this figure. First, the asymmetry parameter β varies rapidly for electron energies near threshold for all subshells, implying rapid variation of either

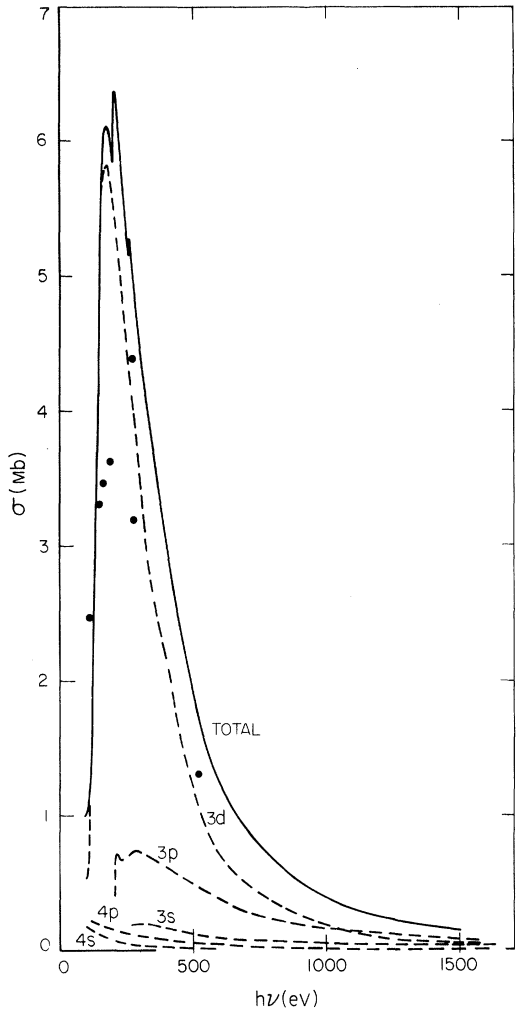

FIG. 1. Total and individual subshell contributions for Kr photo-ionization in the energy range 100–1500 eV. The circles represent experimental data from Ref. 16.

the phase shifts of Eq. (7), or the matrix elements $R_{\epsilon,l\pm1}$, or both.[20] Similar results for photodetachment from negative ions were obtained in Ref. 6. For electron energies close to threshold such rapid variations mean that calculations of the photoionization cross section, and particularly their angular distributions, are model sensitive, and the lack of agreement between our calculations and the measured value of β from Ref. 19 is not surprising.[21]

Second, at energies considerably above threshold the agreement between theory and experiment is satisfactory. Note that the experimental values even show some evidence of the upward trend of $\beta(\epsilon)$ for $3d$ electrons between ~100 and 400 eV. Finally, for $3p$ and $4p$ electrons $\beta(\epsilon)$ is practically the same at energies far from threshold. Again this is to be expected since the phase shifts in Eq. (11) are the same for both subshells within our model and the ratio $R_{\epsilon,l+1}/R_{\epsilon,l-1}$ is approximately the same for both subshells far from threshold.

The above treatment neglects the effect of retardation entirely. In zeroth order Born approximation the angular distribution for an nl subshell electron ejected in photoabsorption by unpolarized light may be related to the bound-state wave function in momentum space by the relation[22]

$$d\sigma_{nl}/d\Omega \sim \sin^2\theta\, F_{nl}^2(|\vec{K}-\vec{K}_\nu|), \tag{9}$$

where $\vec{K}$ and $\vec{K}_\nu$ are the electron and photon propagation vectors, respectively, and F_{nl} is the radial wave function in momentum space.

Evaluation of the form of the angular distribution can be carried out by use of the relation:

$$|\vec{K}-\vec{K}_\nu|^2 \cong K^2[1-(v/c)\cos\theta], \tag{10}$$

where v is the velocity of the ejected electron. The angular distribution may be evaluated by using Eq. (9) with estimates of the function F_{nl}. Then $F_{nl}^2(|K-K_\nu|)$ evaluated by this procedure may be considered as a correction term to the factor $\sin^2\theta$ in Eq. (2).

The above procedure has been used in Ref. 5 to evaluate the form of the angular distribution for s state electrons using hydrogenic radial wave functions, with the additional assumption that the electron energy is high enough that only first order terms in electron energy need be considered. With this approximation the angular distribution for all s-state electrons will be of the form:

$$\frac{d\sigma_{n0}}{d\Omega} \sim \sin^2\theta/[1-(v/c)\cos\theta]^4$$

$$\sim \sin^2\theta\,[1-(4v/c)\cos\theta]\,. \tag{11}$$

This is also the exact result for K shell electrons when hydrogenic wave functions are used. For low energies and outer subshells the use of screened hydrogenic momentum wave functions for each nl subshell provides a better approximation. Here we apply this treatment to the results obtained in Ref. 4, where Mg(K_α) radiation was used to obtain angular distributions for $3s$, $3p$ and $3d$ electrons in Kr. The "radial" momentum wave functions for these subshells are in the hydrogenic approximation[23]

$$F_{30(\rho)} = (144/\sqrt{3\pi})(\rho^2-1)^2/(\rho^2+1)^4 - 1\,, \tag{12}$$

$$F_{31(\rho)} = (144/\sqrt{13\pi})\rho(\rho^2-1)/(\rho^2+1)^4\,, \tag{13}$$

$$F_{32(\rho)} = (288/\sqrt{15\pi})\rho^2/(\rho^2+1)^4;\quad \rho = 3p/Z\,. \tag{14}$$

Here ρ^2 is the electron kinetic energy (in rydbergs) and Z the effective screened charge for the subshell.

For $\rho^2 \gg 1$ the asymptotic form of the square of these functions may be used as an estimate of the corrections produced in the $\sin^2\theta$ term of Eq. (4) by retardation with ρ^2 replaced by $\rho^2[1-(v/c)\cos\theta]$.

The asymptotic forms of Eqs. (12)–(14) are $F_{nl}^2 \sim 1/\rho^{4+l}$.[23] Consequently we expect the correction factors for retardation to be of the form

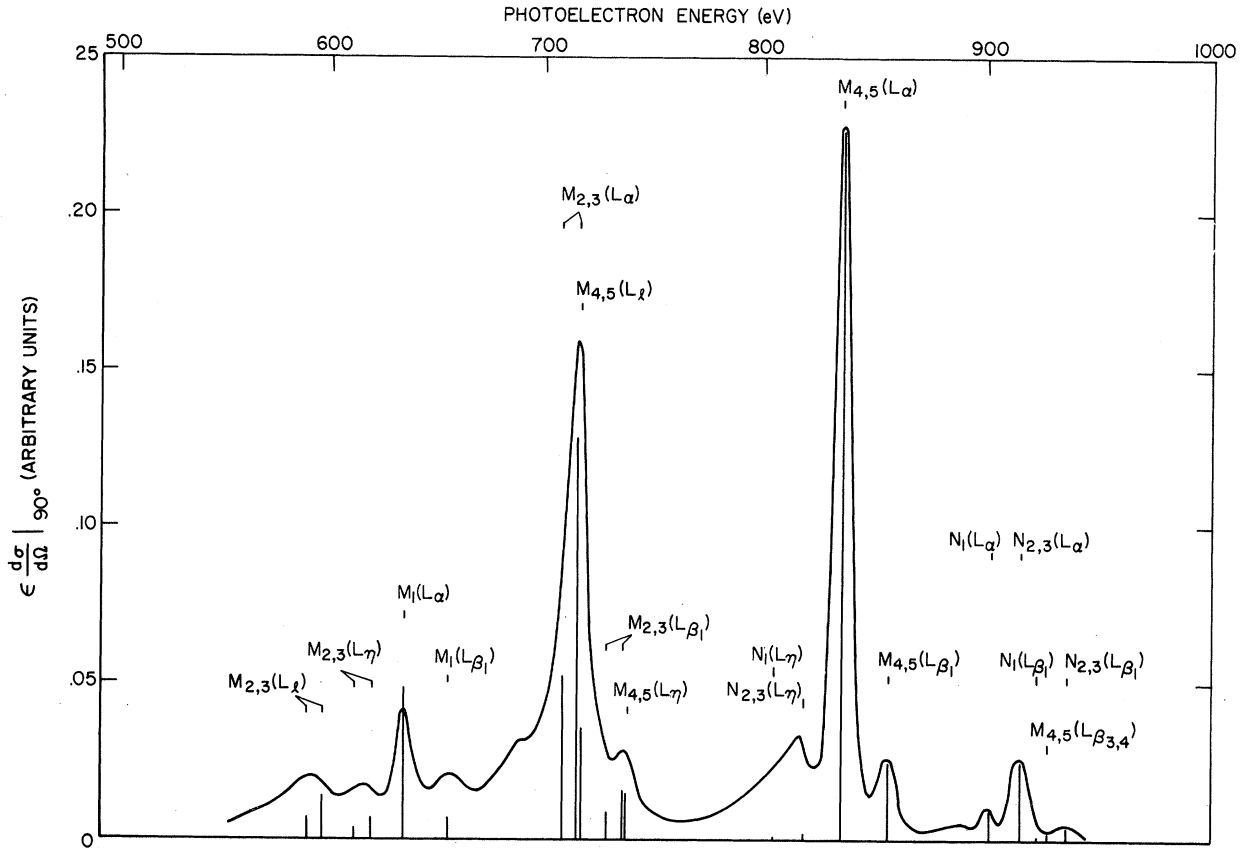

FIG. 2. A comparison of the photoelectron spectra (Fig. 2 of Ref. 4) for a Cu (L) source with calculated values of the individual subshell contributions at 90°. The absolute cross sections calculated for each subshell are weighted by the measured relative intensities of the various lines in the source and multiplied by electron energy. The smooth curve is the experimental spectra and the lines indicate the values of the energy flux at 90° for each subshell component (M_1, M_2, M_3, or $M_{4,5}$) corresponding to each spectral line of the source (e.g. L_α). The experimental curve is normalized to the largest contribution $M_{4,5}$ (L_α).

$[1-(v/c)\cos\theta]^{-4-l}$. At the energies used in Ref. 4, $9p^2/z^2=\rho^2$ is not much greater than unity. Use of Slater screening[24] leads to Z values of 25 for $3s$, 23 for $3p$, and 19 for the $3d$ subshells, and to values of 1.02, 1.3 and 2.1 for ρ^2, respectively, for electrons ejected by Mg(K_α). The value for the $3d$ subshell ($\rho^2=2.1$) is probably large enough that the asymptotic form $[1+6(v/c)\times\cos\theta]$ for the retardation correction is adequate. The data of Ref. 4 is consistent with this result. However, for the $3s$ and $3p$ subshells the asymptotic form is not valid. For the $3s$ subshell and $\rho^2\sim 1$ in Eq. (12), the correction factor is unity to first order in $(v/c)\cos\theta$, again in agreement with the results of Ref. 4, which show little or no shift in the angular distribution due to retardation for the $3s$ subshell. The same does not apply for the $3p$ correction term. Eq. (13) vanishes for $\rho-1$ (this would lead to an isotropic distribution) and the form of the angular distribution will be sensitive to the value of Z used for effective screening for small ρ^2. The sensitivity of the correction factor estimated in this way on the effective value of Z used means that estimates of retardation effects using the simple approach outlined above may be seriously in error. Also, as noted in the Ref. 5 first-order Born approximation may make contributions of the same order of magnitude as the zeroth-order estimates for $l\geq 1$. Nevertheless these estimates indicate that the effects of retardation indicated by the results of Ref. 4 are consistent with what would be expected.

IV. FINAL REMARKS

The preceding section indicates substantial agreement between the findings of Ref. 4 and the theoretical results presented in this paper. This is encouraging since it means that central-field model calculations may be used to obtain estimates of the various subshell contributions and, more important, that further experiments of the type reported in Ref. 4 can be used to obtain additional information in regions close to thresholds, where such calculations are expected to be in error, as well as information on multiple electron processes.

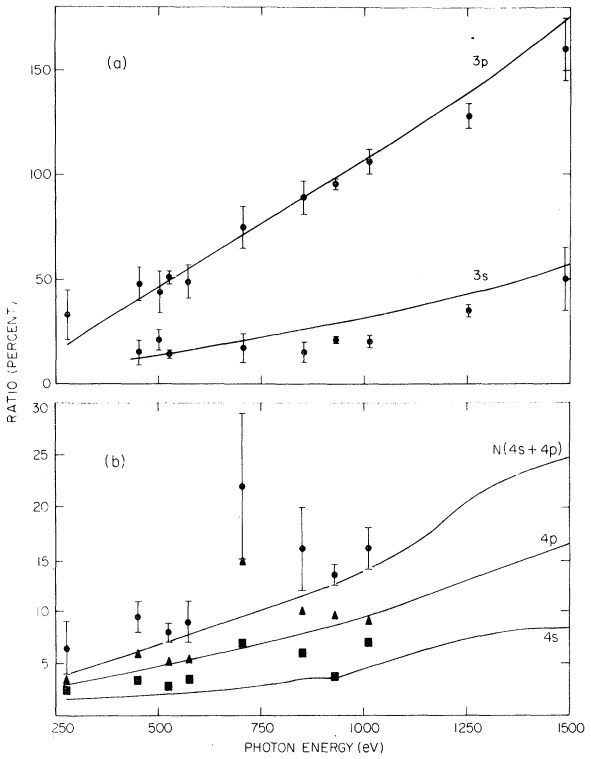

FIG. 3. Ratios of the cross sections for various subshells to the $3d$ cross section (at 90°) versus photon energy. (a) $3p$ and $3s$, (b) $4p$ and $4s$ and their sums. The theoretical ratios are plotted as curves and the experimental values as points with their uncertainties shown as error bars.

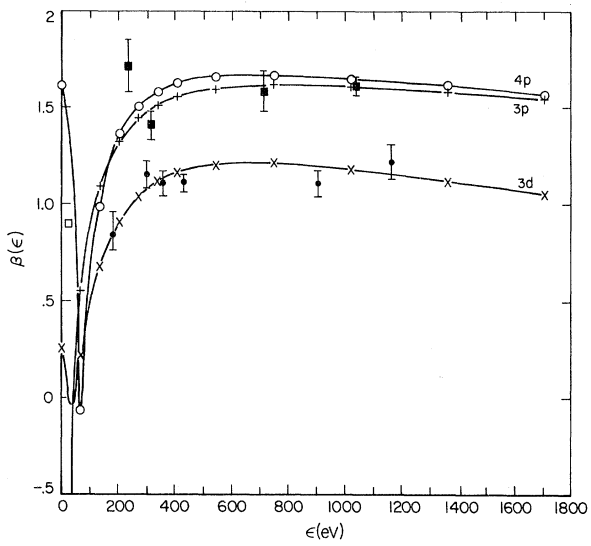

FIG. 4. The asymmetry-parameter (β) for $3d$ (x), $3p$ (+) and $4p$ (0) subshells versus electron energy above threshold. x, + and 0 represent energies at which calculations were carried out. Measured values of β from Ref. 4 for $3p$ (■) and $3d$ (●) subshells are shown with their estimated uncertainties. The results of Ref. 19 for the $4p$ (□) subshell at 584 Å (21.2 eV) is also shown.

The general results presented in Sec. II on the form of the angular distributions in dipole approximation and the discussion of retardation effects in Sec. II and III, do not represent any new physical results. However, we hope this treatment will be useful to experimentalists in planning and interpreting future experiments.

ACKNOWLEDGMENTS

This work was done in close collaboration with Dr. Manfred O. Krause of the Oak Ridge National Laboratory, and would not have been possible without our having had access to his detailed experimental results prior to publication. We also wish to thank Prof. U. Fano for several enlightening discussions on the general form of angular distributions and for constructive comments on the form of this paper.

---

*Postdoctoral Research Associate of the National Academy of Sciences – National Research Council.

†Present Address: Physics Department, Georgia State College, Atlanta, Georgia 30303

[1]Earlier work on electron spectroscopy following photoabsorption has concentrated mainly on determining the ratio of various alternative Auger processes or an accurate determination of the binding energy of inner subshell electrons. For a summary of earlier work see E. H. S. Burhop, The Auger Effect, (Cambridge University Press, New York, 1952), p. 57 *ff*.; and K. Siegbahn, Alpha-, Beta-, and Gamma-Ray Spectroscopy (North-Holland Publishing Co., Amsterdam, 1965).

[2]R. D. Schmickley and R. H. Pratt, Phys. Rev. 164, 104 (1967).

[3]Steven T. Manson and John W. Cooper, Phys. Rev. 165, 126 (1968).

[4]M. Krause, preceding paper, Phys. Rev. 177, 151 (1969). Other work at lower incident energies has also been started. See J. A. R. Samson and R. B. Cairns, Phys. Rev. 173, 80 (1968).

[5]H. A. Bethe and E. E. Salpeter, Quantum Mechanics of One- and Two-Electron Atoms (Academic Press, Inc., New York, 1957), p. 308 *ff*. This work contains references to earlier, more detailed treatments.

[6]J. Cooper* and R. N. Zare, J. Chem. Phys. 48, 942 (1968). We wish to thank these authors for advance notice of their results prior to publication. The asterisk will be used in this manuscript to distinguish Dr. J. Cooper from one of the authors of this paper.

[7]S. Devons and L. J. B. Goldfarb, Handbuch der Physik, edited by S. Flügge (Springer-Verlag, Berlin, 1957), Vol. XLII, p. 362.

[8]Reference 5, pp. 308–310.

[9]J. Cooper* and R. N. Zare, lecture notes of the University of Colorado Theoretical Physics Institute,

1968 (to be published).

[10]C. N. Yang, Phys. Rev. 74, 764 (1948).

[11]B. W. Shore, Rev. Mod. Phys. 39, 439 (1967). In the expansion of the initial photon wave in transverse multipole fields the largest component of angular momentum that can contribute in an electric dipole process corresponds to $L=1$. The first section of Ref. 10 then leads directly to the angular distribution of Eq. (2). Cf. also J. M. Blatt and V. E. Weisskopf, Theoretical Nuclear Physics (John Wiley & Sons, New York, 1952), Chap. XII and Appendix B.

[12]The angular distribution of electrons following electric dipole absorption is somewhat different from the case of scattering by polarized particles [L. Wolfenstein, Phys. Rev. 75, 1664 (1949)]. The same type of reasoning as above leads to a left-right asymmetry in general about the direction of incidence for particles resulting from a collision between polarized particles and unoriented and unpolarized targets. While both photon direction and polarization direction can be specified, the angular distribution of photoelectrons in an absorption process will be independent of photon direction provided absorption is via electric dipole and there will be no asymmetry about the direction of polarization.

[13]The full generality of the results of Ref. 10 depends only on there being no specified orientation of the target particles [A of Eq. (3)] and on the fact that the differential cross section of an single type of outgoing particle is specified. Thus A in Eq. (3) may represent a molecule or nucleus as well as an atom and e may represent any particle emitted as the result of photon absorption. The fact that other particles may also be emitted as a consequence of absorption does not affect the argument since an integration over all coordinates of such particles must be carried out to evaluate the desired differential cross section. Thus Eqs. (1) and (2) give the general form of the differential cross section for any particle that may result from electric dipole absorption.

[14]Within this model each electron is assumed bound in a particular subshell with binding energy ϵ_{nl}. Absorption is treated as a single-electron process in which (electric dipole absorption is assumed) $h\nu=(2me^4/\hbar^2)(\epsilon+\epsilon_{nl})$ defines the final electron energy ϵ where I_t [Eq. (2a)] $=(2me^4/\hbar^2)\epsilon_{nl}$. In this model $\bar{\sigma}(K, I_t)$ and $d\bar{\sigma}(\vec{K}, I_t)/d\Omega$ are defined for each subshell and $\sigma(h\nu)=\Sigma\bar{\sigma}_{nl}(K, I_t)$. As in Ref. 3 the Herman-Skillman potential is the starting point of the calculation.

[15]Equation (8) has an interesting history. It has been derived (Ref. 9) generally, but is also contained implicitly in earlier work by H. A. Bethe [Handbuch der Physik (Springer-Verlag, Berlin, 1933), pp. 482–483] who derived essentially the same expression using hydrogenic wave functions. We would like to thank Dr. Y. K. Kim for pointing out the connection between the recent formulation of Ref. (9) and Bethe's earlier work.

[16]J. A. R. Samson, Advan. Atom. Mol. Phys. 2, 178 (1966).

[17]See also U. Fano and J. W. Cooper, Rev. Mod. Phys. 40, 441 (1968).

[18]One other adjustment has been made in this plot as in Ref. 3, Fig. 2. The experimental binding energies for each subshell rather than the computed values were used to determine the electron energies for each contribution. Also the $M_{2,3}$ component has been split as in Ref. 3.

[19]J. Berkowitz, H. Ehrhardt, and T. Tekaat, Z. Physik 200, 69 (1967).

[20]Typically one expects variations of both $R_{\epsilon, l+1}$ and δ_{l+1} near threshold. For a detailed discussion of this point see Ref. 17, Sec. 4.

[21]A similar discrepancy appears between data for Ar from Ref. 22 and a recent Hartree-Fock calculation, L. Lipsky, in Proceedings of the Fifth International Conference of the Physics of Electronic and Atomic Physics (Nauka, Leningrad, 1967), p. 617.

[22]Equation (9) is obtained from Eq. (70.2) of Ref. 5 by squaring the matrix element, replacing $\cos\theta$ in that expression with $\sin\theta$ and keeping only the radial part of the nlth momentum wave function.

[23]Reference 5, p. 39.

[24]C. Froese, J. Chem. Phys. 45, 1417 (1966).